

# Mesoporous Aluminosilicate of the MCM-41 Type: Its Catalytic Activity in *n*-Hexane Isomerization

K. Chaudhari, T. K. Das, A. J. Chandwadkar, and S. Sivasanker<sup>1</sup>

National Chemical Laboratory, Pune, 411008, India

Received December 18, 1998; revised April 8, 1999; accepted April 19, 1999

Aluminium-containing mesoporous molecular sieves (Al-MCM-41) with different Al contents (Si/Al = 86.3, 43.9, 23.3, and 14.3) have been prepared using cetyltrimethylammonium bromide as an organic surfactant and characterized by XRD, MAS NMR, and N<sub>2</sub> sorption studies. <sup>27</sup>Al NMR studies reveal that the Al is present in Td coordination in the samples. The samples were loaded with Pt and used in the hydroisomerization of *n*-hexane. The reactions were carried out at atmospheric pressure in the temperature range of 300–400°C. The optimum Pt content for the reaction was found to be around 0.3%. High selectivities for isomerization were observed.

© 1999 Academic Press

## INTRODUCTION

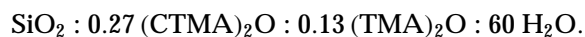
The hydroconversion of *n*-paraffin components of light naphtha into branched isomers is an important process in the petroleum refining industry for obtaining high octane gasoline blendstocks (1, 2). Platinum- or palladium-impregnated zeolites are known to give high isomerization selectivities at medium conversions and are the most common *n*-alkane hydroconversion catalysts. However, due to the strong acidity of these catalysts, their use is characterized by significant hydrocracking to undesirable alkanes at high conversion levels. Since the discovery of siliceous mesoporous molecular sieves (3), designated as M41S and possessing uniform pores whose diameters can be tailored to the desired value (18–100 Å) by the proper choice of synthesis methods, studies of their catalytic properties have become an important aspect of catalysis research. MCM-41 possessing a hexagonal array of pores belongs to the M41S class of molecular sieves. The Al analogs of MCM-41 have been used as solid acid catalysts in a number of acid-catalyzed reactions (4–8). We now report the *n*-hexane hydroconversion activity of Pt-loaded aluminosilicate MCM-41 molecular sieves. We show that Al-MCM-41 molecular sieves possess high isomerization selectivities even at high conversions.

<sup>1</sup> To whom correspondence should be addressed. Fax: +91-20-589-3761; E-mail: siva@cata.ncl.res.in.

## EXPERIMENTAL

### Synthesis of Si-MCM-41

A Si analog of MCM-41 was prepared hydrothermally using a gel with the following molar composition in terms of oxides:



Sodium silicate (28.48% SiO<sub>2</sub>, 9.03% Na<sub>2</sub>O, 62.5% H<sub>2</sub>O), cetyltrimethylammonium bromide (99%, Aldrich), tetramethylammonium hydroxide (TMAOH, 25% aqueous solution, Aldrich), and fumed silica (Cab-O-Sil, 99%, Fluka) were used in the synthesis.

In a typical synthesis, 18.9 g TMAOH was added to 16.86 g sodium silicate diluted with 100 g water. In another beaker 19.68 g CTMABr was dissolved in 50 g water and 30 g ethanol, and 1.9 g aqueous ammonia was added to it (solution A). Solution A was added to the above mixture of sodium silicate and TMAOH and then 7.06 g fumed silica was added to it. The mixture was stirred for 1 h. The gel formed (pH 11.5) was then transferred to an autoclave and heated at 110°C for 5 days. The product was then filtered, washed with distilled water, and dried at ambient temperature. The sample was calcined at 540°C in nitrogen flow for 1 h and then in air for 6 h.

### Synthesis of Al-MCM-41

Al-MCM-41 samples were prepared hydrothermally using a gel with the following molar compositions in terms of oxides,



where  $x \leq 0.08$ . The preparation procedure was similar to that of Si-MCM-41 excepting that sodium hydroxide (0.035 g for Si/Al = 25) dissolved in 8 g water was added to the mixture of sodium silicate and TMAOH and a calculated quantity of Al<sub>2</sub>(SO<sub>4</sub>)<sub>3</sub> · 18 H<sub>2</sub>O (2.52 g for Si/Al = 25) dissolved in 30 g water was added to the final gel and stirred

well. The gel was crystallized as described earlier (110°C for 5 days). Four samples with different Si/Al ratios of 86.3, 43.9, 23.3, and 14.3 (corresponding to input ratios of 100, 50, 25, and 12.5, respectively) were synthesized (Table 1). All the samples were calcined at 540°C in nitrogen flow for 1 h and then in air for 6 h.

The samples synthesized above were characterized by XRD, MAS NMR, and adsorption studies. The calcined samples were converted into the catalytically active H forms by cation exchanging with ammonium nitrate thrice (20 ml of 1 M solution/g of the molecular sieve at 95°C for 5 h), dried at room temperature, and then calcined at 400°C for 6 h.

The platinum loading of H-Al-MCM-41 samples was carried out by impregnation with tetramine platinum (II) nitrate (Aldrich, 99%) to get different Pt loadings (0.1 to 0.5 wt%). After impregnation, the materials were dried in air at 110°C for 4 h, calcined at 400°C for 3 h in air, and reduced at 400°C for 4 h in hydrogen.

### Characterization

The chemical compositions of the samples were determined by X-ray fluorescence technique. The crystalline phase identification and phase purity of the as-synthesized and calcined samples were carried out by XRD (Philips, Holland) using nickel-filtered  $\text{CuK}\alpha$  radiation ( $\lambda = 1.5406 \text{ \AA}$ ). The sorption capacities for  $\text{H}_2\text{O}$ , *n*-hexane, and benzene were measured using a vacuum (Cahn) balance. Prior to sorption measurements, about 200 mg of the sample was activated at 673 K under vacuum. The surface areas and pore diameters were determined from  $\text{N}_2$  adsorption isotherms using a Coulter (Omnisorp 100 CX) instrument.  $^{27}\text{Al}$  MAS NMR spectra of the samples were recorded on a Bruker MSL 300 NMR spectrometer. Temperature-programmed desorption of pyridine was studied on H-Al-MCM-41 and samples under chromatographic conditions (9). The data were collected using a Perkin-Elmer Sigma 3B gas chromatograph with a flame ionization detector. Nitrogen was used as the carrier gas (flow rate,  $40 \text{ cm}^3/\text{min}$ ). The platinum dispersion measurements of the 0.5% Pt-

impregnated H-Al-MCM-41 samples with different Si/Al ratios were carried out by hydrogen chemisorption at ambient temperature (10).

The catalytic reactions were carried out in a down flow fixed-bed tubular glass reactor (i.d. = 15 mm; 30 cm in length) at atmospheric pressure using about 2 g of the catalyst in the presence of hydrogen. *n*-Hexane was fed using a syringe pump and  $\text{H}_2$  was introduced using a mass flow controller. The top section of the reactor (~20 cm long) above the catalyst bed (~3 cm long), which was packed with ceramic beads, acted as the preheating section. The reactor was placed inside a temperature-controlled vertical furnace (Geomécanique, France). The thermocouple tip was centered at the middle of the catalyst bed. The catalyst was compacted in a hydraulic press, and the pellets were broken and then sieved to 16–20 mesh size prior to use. *n*-Hexane used was >99% pure (S.D. Fine Chemicals Pvt., Ltd., Bombay). The conditions of the reactions were as follows: temperature, 300–400°C; WHSV ( $\text{h}^{-1}$ ) = 0.5 to 5.0;  $\text{H}_2/n\text{-C}_6$  (mole) = 2 to 9. The catalyst was dried *in situ* in a flow of  $\text{N}_2$  (20 ml/min) at 450°C for 6 h, cooled to 350°C, and reduced for 2 h in  $\text{H}_2$  (20 ml/min) prior to the start of the run. The reaction products (which were in the gaseous state) were analyzed using a Hewlett-Packard gas chromatograph (5880 A) with a capillary column (cross-linked methyl silicone gum, HP1, 50 m  $\times$  0.2 mm i.d.) and a flame ionization detector.

## RESULTS AND DISCUSSION

### Physicochemical Properties

The XRD patterns of the calcined Al-MCM-41 samples with different Si/Al ratios and the pure silica Si-MCM-41 are presented in Fig. 1. The samples produced relatively well-defined XRD patterns identical to those reported for MCM-41 materials (3, 11, 12). Kresge *et al.* (3) indexed these peaks for a hexagonal unit cell, the parameter of which was calculated from the equation  $a_0 = 2d_{100}/\sqrt{3}$ . The unit cell parameter and *d* spacing of the Al-MCM-41 samples and Si-MCM-41 are given in Table 1. The slight increases

TABLE 1  
Physicochemical Properties of Al-MCM-41 Samples

Samples	Si/Al ratio		$d_{100}$ spacing		Surface area ( $\text{m}^2/\text{g}$ )	Pore volume ( $\text{ml}/\text{g}$ )	Pore diameter ( $\text{Å}$ )
	Input in gel	Calcined sample					
			As-syn.	Calcined			
Si-MCM-41	—	—	36.40	33.00	990	0.60	23
Al-MCM-41(A)	100	86.3	36.48	33.19	1013	0.69	23
Al-MCM-41(B)	50	43.9	37.72	34.48	1025	0.76	24
Al-MCM-41(C)	25	23.3	38.72	35.39	1072	0.79	25
Al-MCM-41(D)	12.5	14.3	39.76	36.48	1098	0.82	26

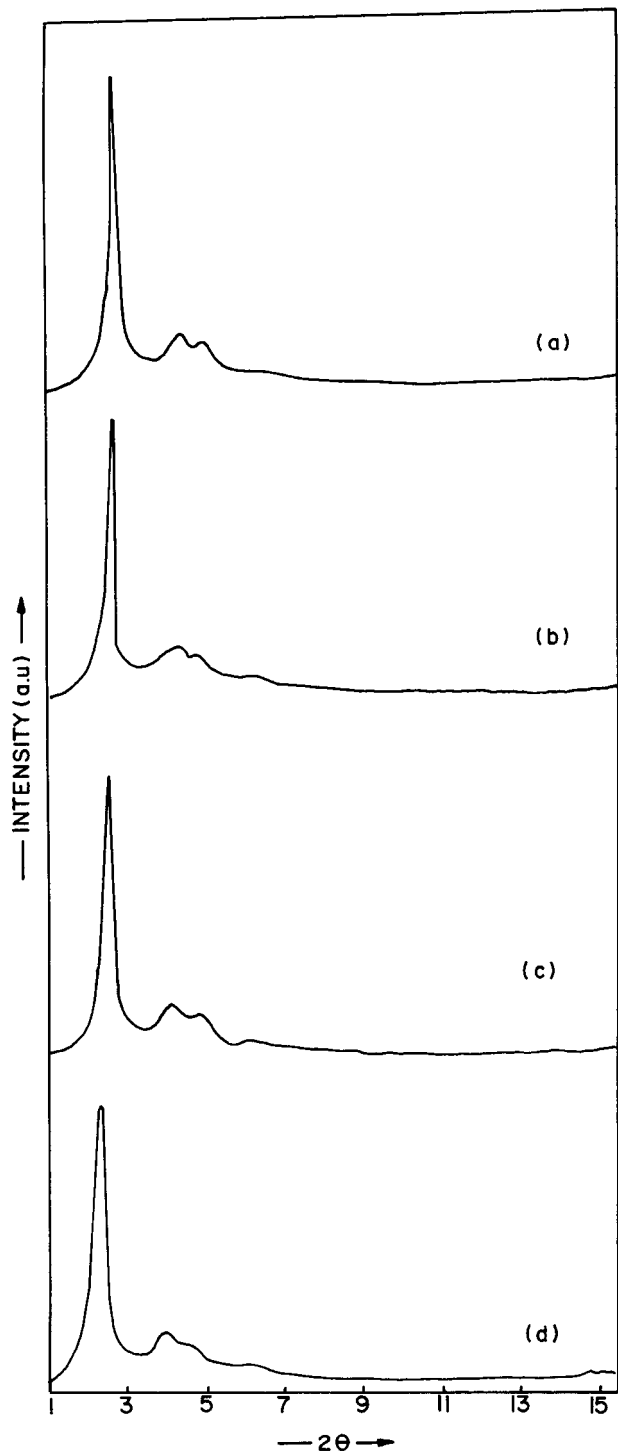


FIG. 1. XRD patterns of calcined samples. (a) Si-MCM-41, (b) Al-MCM-41(B), (c) Al-MCM-41(C), and (d) Al-MCM-41(D).

in *d* spacing and unit cell parameters of Al-MCM-41 compared to its pure silica analog (Table 1) suggest the presence of aluminium in the framework. The increase in unit cell parameter on Al incorporation is probably due to the replacement of shorter Si-O bonds by longer Al-O bonds

in the structure (13). It is also observed that along with an increase in the unit cell parameter, the (100) diffraction peak becomes broader and less intense with increasing aluminium content, probably because of the change in the T-O-T bond angle due to aluminium incorporation causing a distortion in the long-range ordering of the hexagonal mesoporous structure. Similar effects have been observed by earlier workers also (3, 8).

The average pore diameters calculated from N<sub>2</sub> adsorption isotherms using BJH model (14), the BET surface areas, and the pore volumes of the Al-containing samples are presented in Table 1. The isotherms are of type IV (14). The isotherms exhibit three stages, viz., monolayer adsorption of nitrogen on the walls of mesopores ( $p/p_0 < 0.2$ ), the part characterized by a steep increase in adsorption due to capillary condensation in mesopores with hysteresis ( $p/p_0 = 0.15-0.3$ ), and multilayer adsorption on the outer surface of the particles (14). The pore diameters increase with increasing Al content of the samples. The pore volumes calculated (at  $p/p_0 = 0.5$ ) from N<sub>2</sub>, *n*-hexane, and benzene adsorption are nearly similar (Table 2).

The MAS <sup>27</sup>Al NMR spectra of as-synthesized and calcined Al-MCM-41 are presented in Fig. 2. The as-synthesized samples show only a single signal with  $\delta = 54$  ppm due to Al in tetrahedral coordination. No peak at 0 ppm corresponding to octahedral Al species is seen. The <sup>27</sup>Al signals of the Al-MCM-41 samples are found to be broader than the signals generally observed for zeolitic Al, presumably due to the presence of greater distortions in the tetrahedral environment. On calcination, additional very low intensity signals are seen at  $\sim 32$  ppm attributable to Al<sup>3+</sup> ions in nontetrahedral coordination in the case of the sample with the highest Al content (Al-MCM-41(D)) (Fig. 2f).

The acidities of the H-Al-MCM-41 samples were characterized by the TPD of pyridine. The acid strengths appear to be rather moderate as nearly all the pyridine desorbed below 300°C. The acidities (mmole/g) based on the pyridine desorbed by the samples beyond 100°C are presented in

TABLE 2  
Pore Volume, Acidity, and Pt Dispersion of the Samples

Sample	Pore volume (ml/g)			Acidity (mmole/g) <sup>b</sup>	Dispersion D (H/Pt) <sup>c</sup>
	<i>n</i> -Hexane	Benzene	N <sub>2</sub> <sup>a</sup>		
Si-MCM-41	0.68	0.64	0.60	—	—
Al-MCM-41(A)	0.70	0.75	0.69	0.035	0.74
Al-MCM-41(B)	0.73	0.72	0.76	0.060	0.69
Al-MCM-41(C)	0.74	0.75	0.79	0.098	0.78
Al-MCM-41(D)	0.76	0.77	0.82	0.152	0.64

<sup>a</sup> Calculated from N<sub>2</sub> adsorption isotherm at liquid nitrogen temperature.

<sup>b</sup> Pyridine desorbed beyond 100°C.

<sup>c</sup> Pt content was 0.5 wt% for all samples.

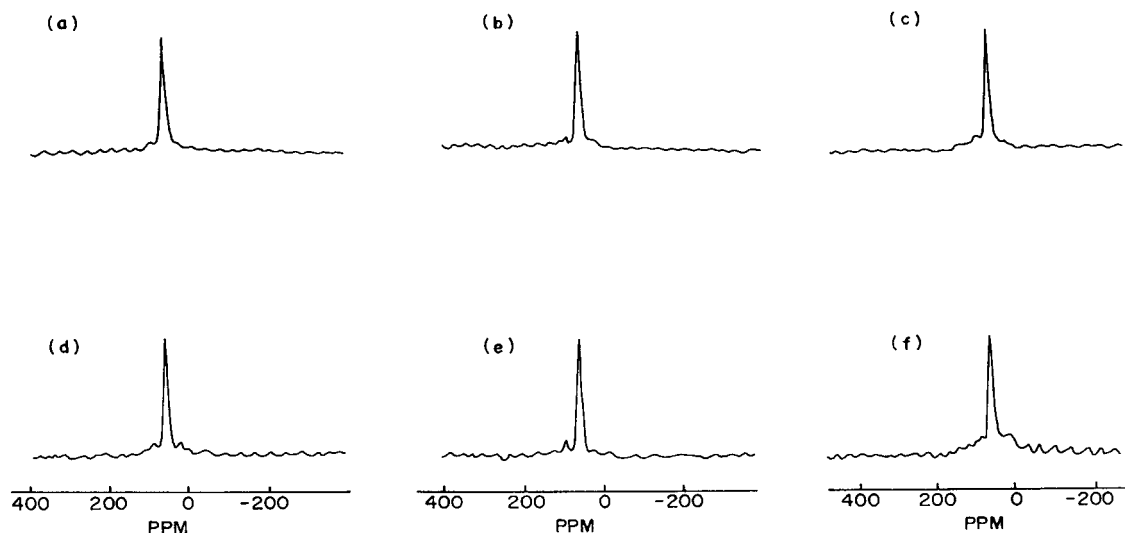


**FIG. 2.**  $^{27}\text{Al}$  MAS NMR spectra of the samples. As-synthesized: (a) Al-MCM-41(A), (b) Al-MCM-41(C), and (c) Al-MCM-41(D); calcined: (a) Al-MCM-41(A), (b) Al-MCM-41(C), and (c) Al-MCM-41(D).

Table 2. As the aluminium content increases, the total acidity increases in the samples (Al-MCM-41(A) < Al-MCM-41(B) < Al-MCM-41(C) < Al-MCM-41(D)).

The Pt dispersion values of the Pt-H-Al-MCM-41 samples determined by hydrogen chemisorption are presented in Table 2. The Pt dispersions were almost similar for all the samples (64 to 78%).

#### Transformation of *n*-Hexane

Hydroisomerization of alkanes is generally carried out over bifunctional catalysts, often containing platinum. The metal component aids in increasing the rate of isomerization, besides lowering catalyst deactivation. The reactivity of *n*-alkanes increases as the carbon number increases but the selectivity toward isomerization decreases (15). The hydroisomerization of *n*-hexane has already been studied over Pt-loaded zeolites such as Pt-Y (16), Pt-beta (17), and Pt-mordenite (18). There is a general consensus on the mechanism of alkane hydroisomerization. *n*-Alkane molecules are adsorbed at dehydrogenation/hydrogenation sites where *n*-alkenes are formed. These migrate and interact with acid sites and secondary carbenium ions are generated, which further rearrange to more stable tertiary carbenium ions. Finally, the tertiary carbenium ions abstract hydride ions from hydrocarbon molecules and transform into olefins. These are then hydrogenated at the metallic sites into isoalkanes (19, 20).

The hydroconversion of *n*-hexane was carried out by us in a fixed-bed down flow glass reactor at atmospheric pressure in the temperature range of 300–400°C over Pt-H-Al-MCM-41 samples containing different amounts of Pt (0.1–

0.5 wt%). Under the conditions of the investigation, the major reactions were isomerization and cracking; negligible cyclization and aromatization were observed. Small amounts of alkenes (1–2%) were also detected in the products. In this paper, the activities of catalysts (Figs. 3–8) are expressed as conversion (%) and turnover frequencies (TOF,  $\text{s}^{-1}$ ) based on the number of acid sites as estimated from temperature-programmed desorption of pyridine (Table 2). A decrease in *n*-hexane conversion (and TOF) was observed with duration of run (time on stream, TOS) over all the catalysts. Though the deactivation rate was significant during the first few minutes (Fig. 3), the activity of the catalyst became reasonably stable after about 45 min. Hence the data reported were collected at a TOS of 45 min during further studies of the reaction. A certain amount of initial deactivation has also been reported by other workers during the isomerization of *n*-alkanes over Pt catalysts (16, 21), which is expected under atmospheric pressure conditions.

**Influence of Pt content.** The influence of Pt content on the hydroisomerization of *n*-hexane over Pt-H-Al-MCM-41 (Si/Al = 23.3) (Pt-H-form of Al-MCM-41(C)) at different temperatures is presented in Fig. 4a. The incorporation of Pt increases the activity of H-Al-MCM-41 severalfold (Fig. 4a). The conversion increases rapidly with increasing Pt content up to about 0.2% and slowly thereafter. This behavior is typically noticed when a bifunctional mechanism is the major contributor to the reaction (19, 22, 23). The selectivity of the catalysts for the isomerization reaction can be evaluated by the relative amount of the isomerization and cracking products formed in the reaction, which can be

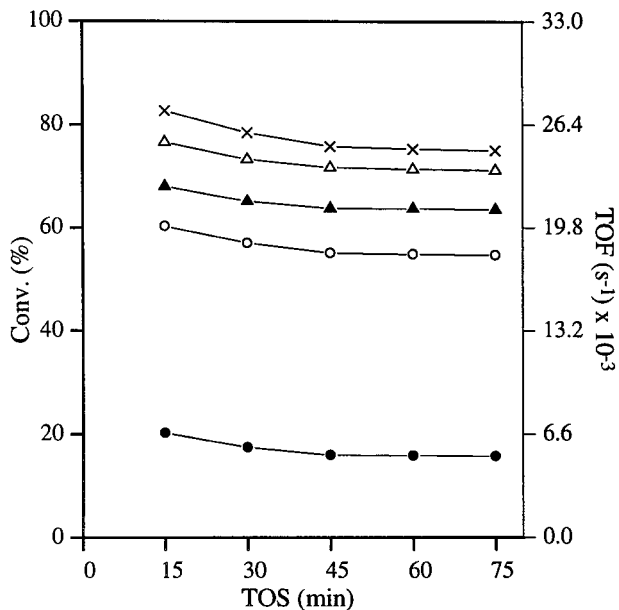


FIG. 3. Influence of time on stream (TOS) on activity of catalyst. Catalyst, Pt(0.3%)-Al-MCM-41(C); WHSV ( $\text{h}^{-1}$ ) = 1.0;  $\text{H}_2/n$ -hexane (mole) = 3.5. (●) 300°C, (○) 325°C, (▲) 350°C, (△) 375°C, and (×) 400°C.

conveniently expressed by the  $I/C$  (isomerization/cracking) ratio.

The influence of Pt content on the selectivity to isomerization is shown in Fig. 4b. The  $I/C$  ratio increases with increase in Pt content and reaches a maximum at about 0.3 wt% Pt ( $I/C = 65$  at a conversion of  $\sim 55\%$  at 325°C). The  $\text{C}_1$ - $\text{C}_5$  fraction increases with increasing Pt content (Fig. 4c) due primarily to an increase in the hydrogenolysis activity which is confirmed by the increase in the  $\text{C}_1 + \text{C}_5/\text{C}_3$  ratio (Fig. 4d). Apparently, the enhanced hydrogenolysis activity is the main reason for the decrease in  $I/C$  ratio beyond 0.3% Pt. The distribution of isohexane is shown in Fig. 4c and the ratios of the products are presented in Fig. 4d. When Pt is present (even 0.1%) the ratios of the monomethylpentanes (2-MP/3-MP) (1.52 to 1.65) are close to the expected equilibrium value of 1.57 (19) suggesting the rapid equilibration of the two isomers; in the absence of Pt, the equilibrium is not attained (2-MP/3-MP = 2.2). The ratios of methylpentanes/dimethylbutanes (MP/DMB) are, however, far from the equilibrium value (3.51), being  $\sim 6$  when Pt is present and 14.8 when absent, due to the difficulty in the isomerization of the methylpentanes to dimethylbutanes. The 2,3-DMB/2,2-DMB ratios decrease (2.0 to 0.84) with increasing Pt content and reach the equilibrium value of 0.86 at 0.5% Pt. The results suggest that the metal function, besides acting as the hydrogenation-dehydrogenation agent, probably also assists the isomerization of the carbocation, though it is not clear how.

**Influence of Si/Al ratio.** The influence of Al content in the Pt-H-Al-MCM-41 samples was studied at 325 and 350°C

with catalysts having different Si/Al ratios (Si/Al ratios of 86.3, 43.9, 23.3, and 14.3) impregnated with 0.3 wt% Pt. The conversion decreases with decreases in Al content; i.e., the higher the Si/Al ratio the lower is the conversion (Figs. 5a and 5c). The activity of a commercial silica alumina cracking catalyst (LA-LPV; Ketjen; S.A. =  $650 \text{ m}^2/\text{g}$ ) at 325 and 350°C is also presented in Figs. 5a and 5c. The amorphous silica alumina sample is relatively less active for the given Al content, probably due to a poor distribution of Al. Both cracking and isomerization are enhanced with increasing Al content. However, the  $I/C$  ratio peaks for the sample with an intermediate Si/Al value (23.3). Though the reasons for this behavior are not clear, it is probably connected with the presence of some very strong acid centers in samples with low and high Si/Al ratios. While strong acidity in the Si-rich samples (Al-MCM-41(A); Si/Al = 86.3) may be due to the extreme isolation of Al ions, it could be due to the presence of small amounts of extra framework Al species in the Al-rich sample (Al-MCM-41(D); Si/Al = 14.3).

It is also possible that the above behavior is due to the different  $n_{\text{Pt}}/n_{\text{A}}$  ( $n_{\text{Pt}}$  = no. of exposed Pt atoms and  $n_{\text{A}}$  = no. of acid sites) in the samples. For example, when the  $n_{\text{Pt}}/n_{\text{A}}$  is large, hydrogenolysis activity will be predominant. When it is very small, the acid activity (cracking) will prevail; isomerization (bifunctional reaction) selectivity will be maximum when the ratio of the two functions is optimum. The distribution of the light products from the samples is not typical of either hydrogenolysis or cracking, as more (moles of)  $\text{C}_4$  and  $\text{C}_5$  hydrocarbons are present than can be accounted for by yields of  $\text{C}_1$  and  $\text{C}_2$  hydrocarbons. Similar imbalance has also been reported by earlier workers (18) and attributed to the occurrence of alkylation-cracking reactions during alkane transformations over metal-loaded zeolites. Earlier, Guisnet *et al.* (24) have reported while studying Pt-H-Y that acid activity becomes important when  $n_{\text{Pt}}/n_{\text{A}}$  is  $< 0.03$  and hydrogenolysis activity becomes important when  $n_{\text{Pt}}/n_{\text{A}}$  is  $> 0.4$ . Unlike in the case of Y, it is difficult to estimate the number of acid sites in H-Al-MCM-41 based only on the Al content. Besides, the acid sites in H-Al-MCM-41 are much weaker than those in zeolites (25). It is therefore difficult to arrive at the exact  $n_{\text{Pt}}/n_{\text{A}}$  ratios for our catalysts. Our studies on the TPD of pyridine over the Pt-H-Al-MCM-41 samples revealed that most of the pyridine desorbed before 300°C, attesting to the weak nature of the acid centers. An estimate of the acid sites based on pyridine desorbed beyond 100°C is presented in Table 2. Assuming that each acid site desorbs a single pyridine molecule (Table 2), and assuming an average Pt dispersion of 70%, we obtain  $n_{\text{Pt}}/n_{\text{A}}$  values in the range of 0.06 to 0.42 for Si/Al (86.3 to 14.6) in the samples at constant Pt (0.3%) and in the range 0.036 to 0.18 for Al-MCM-41(C) with different Pt contents (0.1 to 0.5%). Both sets of studies (Si/Al and Pt content variations) suggest a maximum isomerization selectivity for Sample C with 0.3% Pt with an  $n_{\text{Pt}}/n_{\text{A}}$  ratio of 0.11 (Figs. 4b

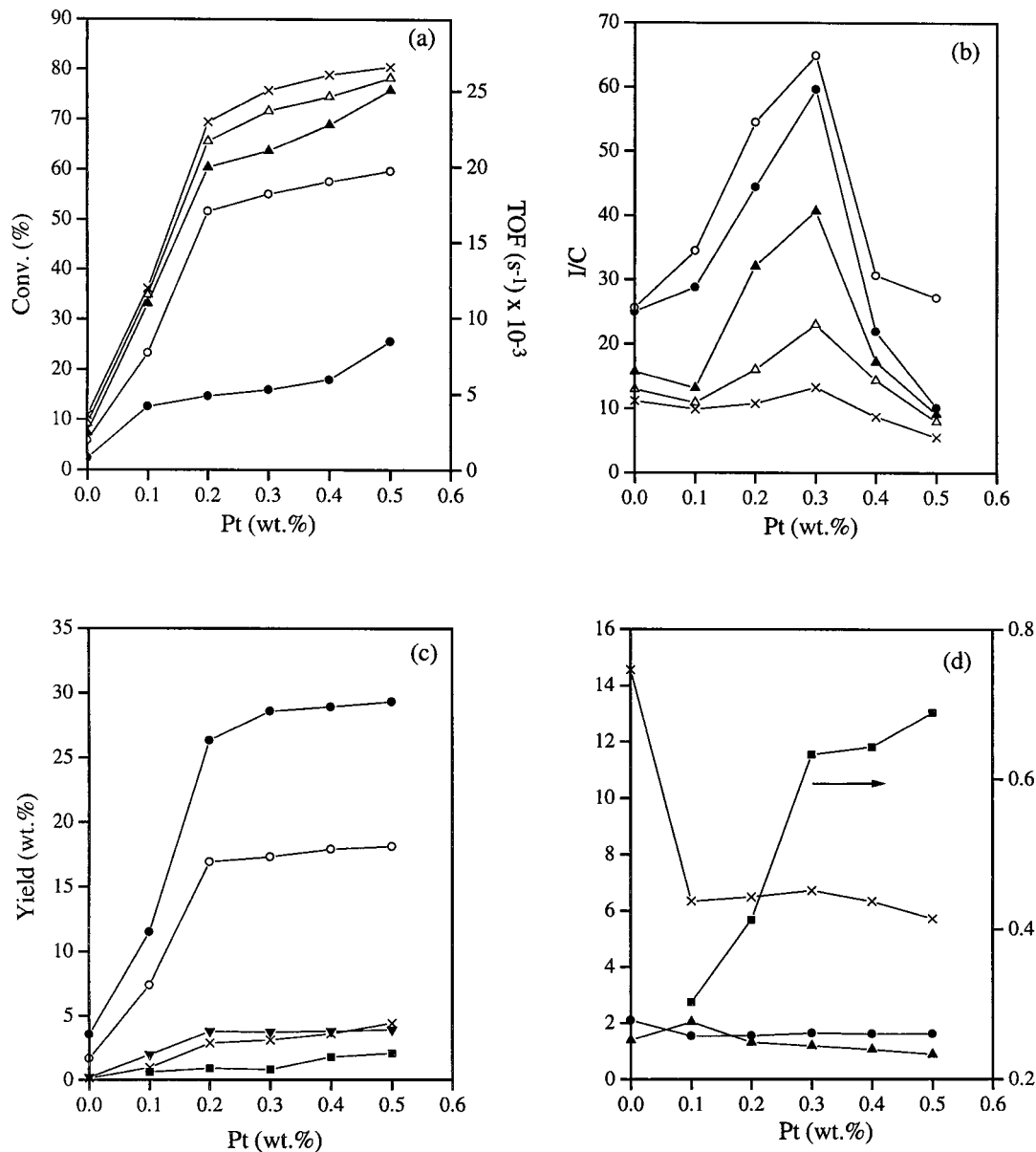


**FIG. 4.** Influence of Pt content on *n*-hexane isomerization. Catalyst, Pt-Al-MCM-41(C) with different Pt contents; WHSV ( $\text{h}^{-1}$ ) = 1.0;  $\text{H}_2/n$ -hexane (mole) = 3.5; TOS = 45 min. (a) and (b): (●) 300°C, (○) 325°C, (▲) 350°C, (△) 375°C, and (×) 400°C; (c): (●) 2-MP, (○) 3-MP, (▼) 2,3-DMB, (×) 2,2-DMB, and (■)  $\text{C}_1$ - $\text{C}_5$  products; (d): (●) 2-MP/3-MP, (▲) 2,3-DMB/2,2-DMB, (×) MP/DMB, and (■)  $\text{C}_1 + \text{C}_5/\text{C}_3$ .

and 5a). This value is within the limit reported by Guisnet *et al.* (24).

**Influence of temperature.** The influence of temperature on *n*-hexane transformation over Al-MCM-41(C) with different Pt contents is presented in Fig. 6a. Though the activities of the catalysts increase with temperature, the increase is moderate beyond 350°C. This is mainly due to the near attainment of equilibrium for the isomerization reaction at higher temperatures. The theoretical equilibrium conversion (isomerization) values (based on data of Ref. 26) are also presented in the Fig. 6. Due to the occurrence of side

reactions such as cracking and hydrogenolysis which are not *equilibrium limited*, the conversion recorded by us is generally lower than the equilibrium values even at temperatures above 350°C. The activation energies ( $E_a$ ) for isomerization calculated for the different samples based on the data collected below 325°C (at low conversions away from the equilibrium values) were in the range 22–31 kcal mole $^{-1}$  (22 kcal mole $^{-1}$  for 0.2% Pt and 31 kcal mole $^{-1}$  for 0.5% Pt). The  $E_a$  values for cracking (and hydrogenolysis) were in the range 15–22 kcal mole $^{-1}$  in the entire temperature range (22 kcal mole $^{-1}$  for 0.2% Pt and 15 kcal mole $^{-1}$  for 0.5% Pt). These  $E_a$  values for isomerization and cracking

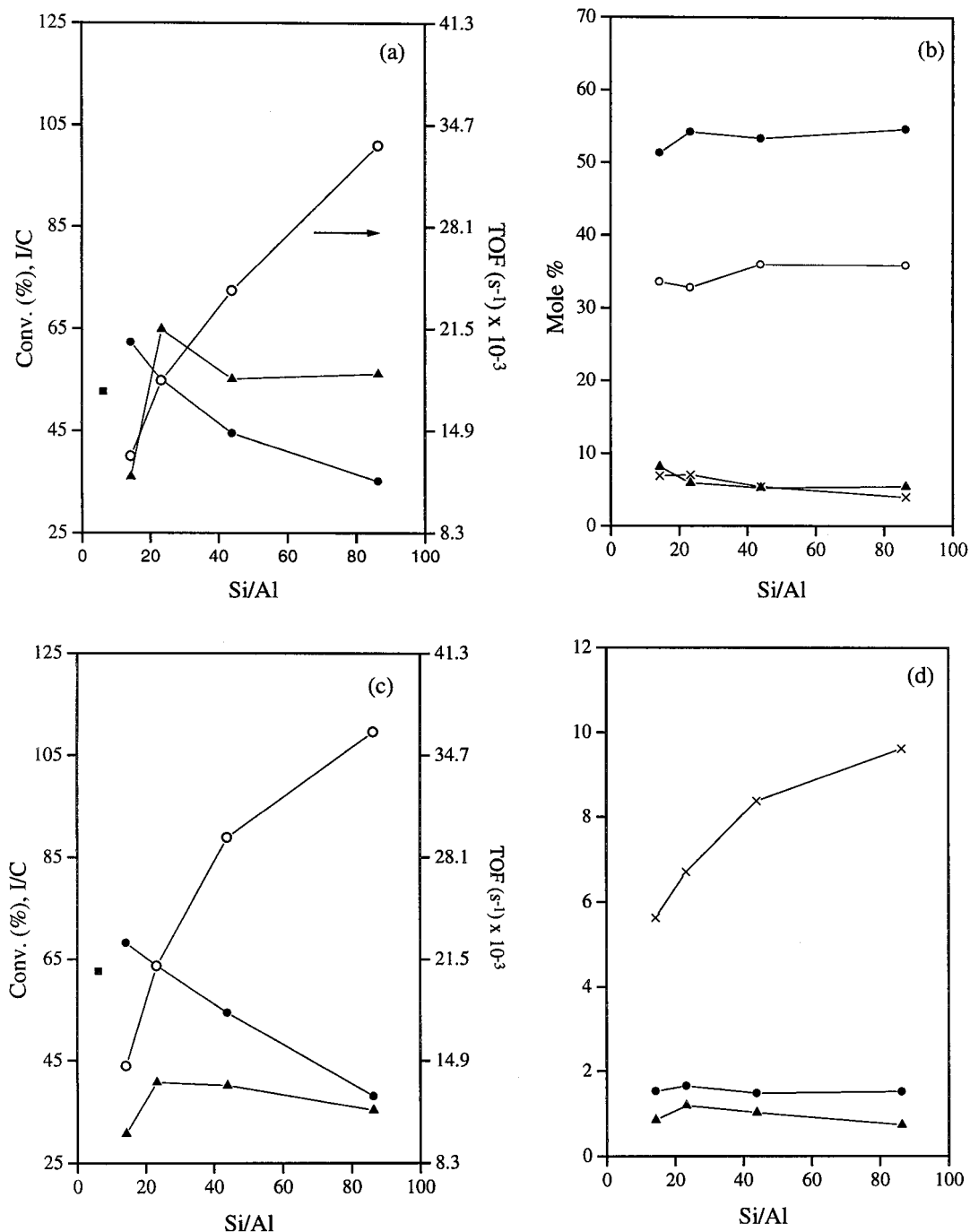


**FIG. 5.** Influence of Al content on *n*-hexane isomerization. Pt-Al-MCM-41(A to D); Pt content = 0.3%; WHSV ( $\text{h}^{-1}$ ) = 1.0;  $\text{H}_2/n$ -hexane (mole) = 3.5; TOS = 45 min. (a) Temperature, 325°C, (●) Conv. (%), (○) TOF ( $\text{s}^{-1}$ ), and (▲) *I/C*; (b) temperature, 325°C, (●) 2-MP, (○) 3-MP, (▲) 2,3-DMB, and (×) 2,2-DMB; (c) temperature, 350°C, (●) Conv. (%), (○) TOF ( $\text{s}^{-1}$ ), (▲) *I/C*, and (■) amorphous  $\text{SiO}_2\text{-Al}_2\text{O}_3$ , % conversion; (d) temperature, 325°C, (●) 2-MP/3-MP, (▲) 2,3-DMB/2,2-DMB, and (×) MP/DMB.

are similar to the values reported by earlier workers (21, 23, 27). However, at higher conversions ( $>325^\circ\text{C}$ ), the  $E_a$  values for isomerization were lower (5–10 kcal mole $^{-1}$ ). This is attributed to the near attainment of equilibrium under these conditions.

The *I/C* ratio goes through a maximum for all the catalysts with different Pt contents (Fig. 6b). The maximum *I/C* obtained is 65% at 325°C (conversion ~55%) with the sample impregnated with 0.3 wt% Pt. The presence of an optimum temperature suggests that the bifunctional

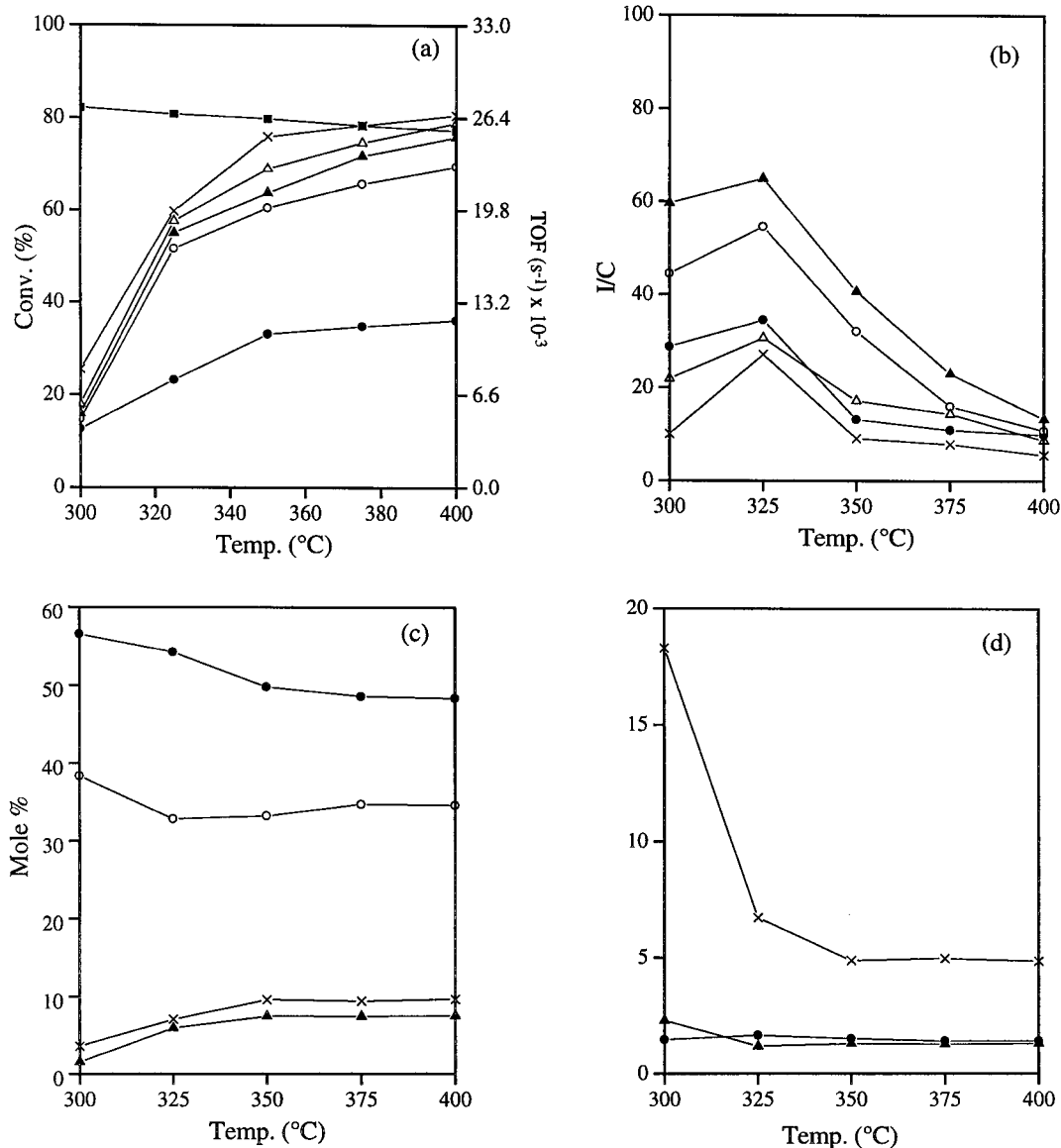


**FIG. 6.** Influence of temperature on *n*-hexane isomerization. Pt(0.3%)-Al-MCM-41(C); WHSV (h<sup>-1</sup>) = 1.0; H<sub>2</sub>/*n*-hexane (mole) = 3.5; TOS = 45 min. (a) and (b) (●) 0.1 wt% Pt, (○) 0.2 wt% Pt, (▲) 0.3 wt% Pt, (△) 0.4 wt% Pt, and (×) 0.5 wt% Pt; (c) (●) 2-MP, (○) 3-MP, (▲) 2,3-DMB, and (×) 2,2-DMB; (d) (●) 2-MP/3-MP, (▲) 2,3-DMB/2,2-DMB, and (×) MP/DMB. The equilibrium conversion (■) values are presented in (a).

activity of the catalyst overrides the other reactions (mono-functional hydrogenolysis or cracking) at this temperature. The break up of the individual components and their ratios at 0.3% Pt content are presented in Figs. 6c and 6d. The 2-MP/3-MP ratio is nearly constant at ~1.6 at all the temperatures, revealing the attainment of equilibrium between the two isomers. The dimethylbutane fraction in the product increases sharply at 325 °C and remains nearly constant (relative to other isomers) (Fig. 6c). This results in a sharp decline in the MP/DMB ratios at 325 °C. The ratio however is still far (4.8) from the equilibrium value (of 3.5) even at 400 °C. However, the 2,3-DMB/2,2-DMB ratio is close to the equilibrium value of 0.86. This confirms

that the nonattainment of the equilibrium between the mono and dimethyl isomers is mainly due to the successive cracking of the dibranched isomers.

**Influence of space velocity.** As the contact time (1/ WHSV) increases, *n*-hexane conversion increases, but the *I/C* ratio decreases (Fig. 7a). The decrease in *I/C* is a result of the increase in cracking reactions favored by the longer residence of the adsorbed intermediates at the surface at the low feed rates. Plots of the yields of the different isomers against conversion (Fig. 7c) suggest that the methylpentanes are the primary products and the dimethylbutanes are the secondary products. The sequence of reactions

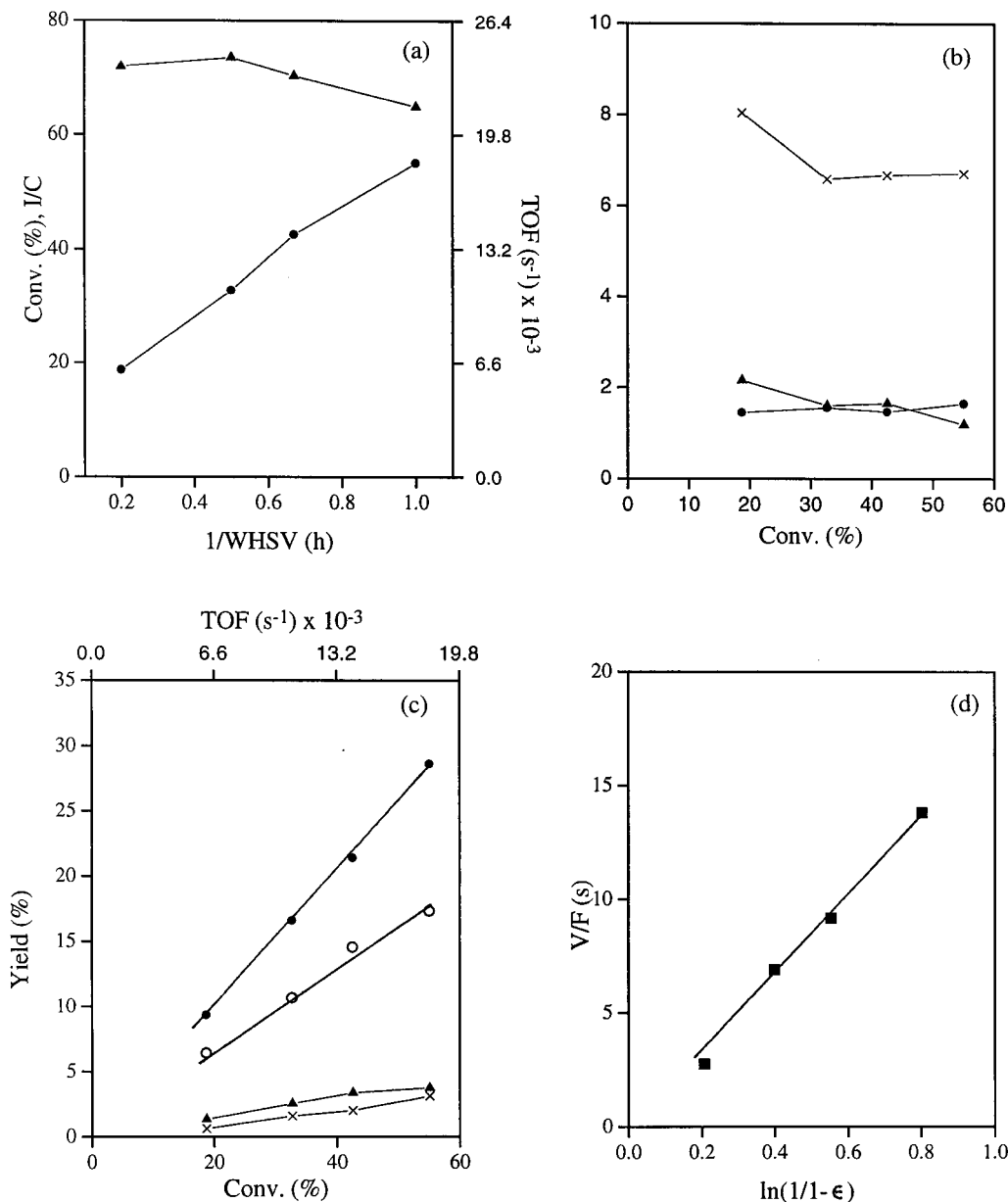


FIG. 7. Influence of space velocity on *n*-hexane isomerization. Pt(0.3%)-Al-MCM-41(C); WHSV (h<sup>-1</sup>) = 1.0; H<sub>2</sub>/*n*-hexane (mole) = 3.5; TOS = 45 min. (a) (●) Conv. (%) and TOF (s<sup>-1</sup>); (▲) I/C; (b) (●) 2-MP/3-MP, (▲) 2,3-DMB/2,2-DMB, and (x) MP/DMB; (c) (●) 2-MP, (○) 3-MP, (▲) 2,3-DMB, and (x) 2,2-DMB; (d) V/F (ln 1/(1 - ε)); first-order kinetics.

is *n*-hexane ⇒ methylpentanes ⇒ dimethylbutanes. Even-though 2,2-DMB is the thermodynamically more favored product under the conditions of the study, its formation (directly from methylpentanes or from 2,3-DMB) is kinetically less favored due to the difficulty in transforming a more stable tertiary carbocation (c-c<sup>+</sup>-c-c-c or c-c-c<sup>+</sup>-c) into a less stable secondary carbocation (c-c-c<sup>+</sup>-c) (19).

The data from the above experiments suggest a first-order kinetics for the conversion of *n*-hexane. This conclusion is arrived at based on the linear  $\delta$  relationship (Fig. 7d)

between  $V/F$  and  $\ln[1/(1 - \epsilon)]$ ;  $k = (1/T) \ln[1/(1 - \epsilon)]$ , where  $P = V/F$ ,  $V$  = volume of the catalyst,  $F$  = feed rate per second, and  $\epsilon$  = fractional conversion (28).

**Influence of H<sub>2</sub>/*n*C<sub>6</sub> mole ratio.** The influence of the H<sub>2</sub>/*n*-C<sub>6</sub> mole ratio is shown in Fig. 8a. Increasing the mole ratio from 2 to 9 ( $P_{H_2} = 0.67$  to 0.90) at a constant feed rate of *n*C<sub>6</sub> decreases the conversion. The decrease in activity with increasing partial pressure of H<sub>2</sub> can be a result of the rapid hydrogenation of the intermediate olefins and carbocations preventing their further reaction. This is clear from a comparison of data obtained from contact time and the

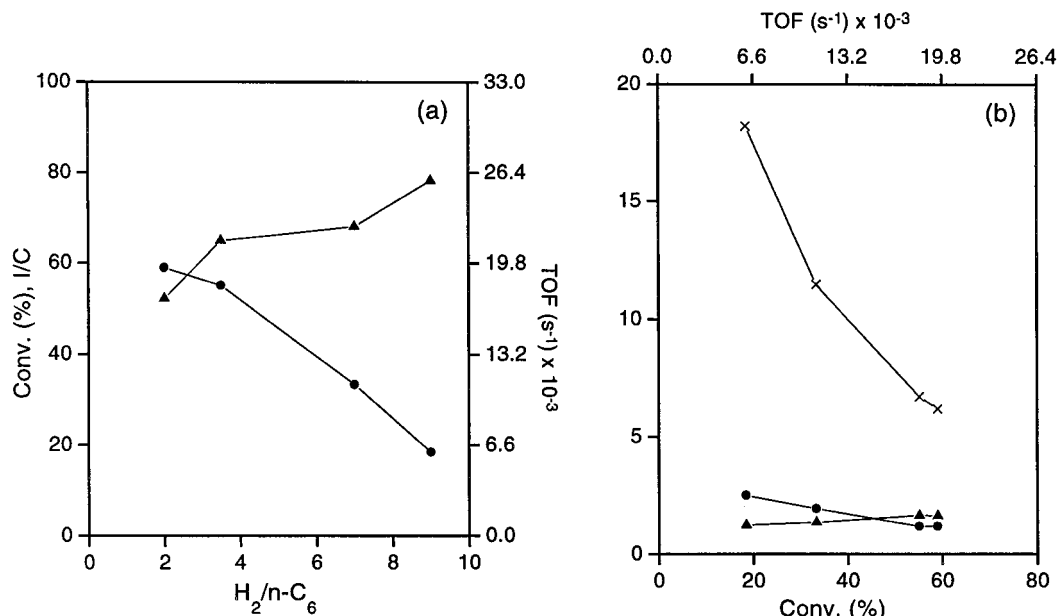


FIG. 8. Influence of  $H_2/n-C_6$  (mole) ratio on  $n$ -hexane isomerization. Pt(0.3%)-Al-MCM-41(C);  $H_2/n$ -hexane (mole) = 3.5; TOS = 45 min. (a) (●) Conv. (%) and (▲) I/C; (b) (●) 2-MP/3-MP, (▲) 2,3-DMB/2,2-DMB, and (×) MP/DMB.

$H_2$  partial pressure studies. For example, at a conversion of about 19%, the MP/DMB ratio is 8.0 in contact time variation experiments ( $P_{H_2} = 0.78$ ), while it is 18 at a similar conversion (18%;  $P_{H_2} = 0.90$ ).

## CONCLUSIONS

Mesoporous aluminosilicates of the MCM-41 type can be prepared by hydrothermal methods. A slight increase in pore width is noticed with increasing Al content. These materials possess  $Al^{3+}$  ions in Td coordination and are moderately acidic. The isomerization of  $n$ -hexane takes place with high selectivities over the Pt-Al-MCM-41 samples. The conversion of  $n$ -hexane follows a first-order kinetics. As is typical of bifunctional catalysis, maximum isomerization selectivity is noticed at an optimum metal to acid site ratio.

## REFERENCES

- Ciapetta, F. G., and Wallace, D. N., *Catal. Rev.* **5**, 67 (1971).
- Cusher, N. A., Greenouch, P., Rolfe, J. P. K., and Weiszmann, J. A., in "Handbook of Petroleum Refining Processes" (R. A. Meyers, Ed.), Chap. 5, p. 5.1. McGraw-Hill, New York, 1986.
- Kresge, C. T., Leonowicz, M. E., Roth, W. J., and Vartuli, J. C., U.S. Patent 5098684, 1992.
- Beck, J. S., and Vartuli, J. C., *Curr. Opin. Solid State Mater. Sci.* **1**, 76 (1996).
- Climent, M. J., Corma, A., Iborra, S., Navarro, M. C., and Primo, J., *J. Catal.* **161**, 783 (1996).
- Girgis, M. J., and Tsao, Y. P., *Ind. Eng. Chem. Res.* **35**(2), 386 (1996).
- Mokaya, R., Jones, W., Moreno, S., and Poncelet, G., *Catal. Lett.* **49**, 87 (1997).
- Chen, X., Huang, L., Ding, G., and Li, Q., *Catal. Lett.* **44**, 123 (1997).
- Nayak, V. S., Ph.D. thesis, University of Poona, Poona, India, 1982.
- Smirniotis, P. G., and Ruckenstein, E., *Appl. Catal.* **123**, 59 (1995).
- Kresge, C. T., Leonowicz, M. E., Roth, W. J., Vartuli, J. C., and Beck, J. S., *Nature* **359**, 710 (1992).
- Beck, J. S., Vartuli, J. C., Roth, W. J., Leonowicz, M. W., Scmitt, K. D., Chu, C. T. W., Olson, D. H., Sheppard, E. W., McCullian, S. B., Higgins, H. B., and Shlenker, J. S., *J. Am. Chem. Soc.* **114**, 10,834 (1992).
- Borade, R. B., and Clearfield, A., *Catal. Lett.* **31**, 267 (1995).
- Gregg, S. J., and Sing, K. S. W., "Adsorption, Surface Area and Porosity," Chap. 4. Academic Press, London, 1982.
- Farneth, W. E., and Gorte, R. J., *Chem. Rev.* **95**, 615 (1995).
- Gianetto, G. E., Perot, G. R., and Guisnet, M. R., *Ind. Eng. Chem. Prod. Res. Dev.* **25**, 481 (1986).
- Leu, L. J., Hou, L.-Y., Kang, B.-D., Li, C., Wu, S.-T., and Wu, J.-C., *Appl. Catal.* **69**, 49 (1991).
- Guisnet, M., Fouche, V., Belloum, M., Bournonville, J. P., and Travers, C., *Appl. Catal.* **71**, 283 (1991).
- Chen, J. K., Martin, A. M., Kim, Y. G., and John, V. T., *Ind. Eng. Res.* **27**, 401 (1988).
- Guisnet, M., Fouche, V., Belloum, M., Bournonville, J. P., and Travers, C., *Appl. Catal.* **71**, 295 (1991).
- Ravishankar, R., and Sivasanker, S., *Appl. Catal. A: General* **142**, 47 (1996).
- Weisz, P. B., *Adv. Catal.* **13**, 137 (1962).
- Jacobs, P. A., Uytterhoeven, J. B., Steijns, M., Foment, G., and Weitkamp, J., in "Proceedings, 5th International Conference on Zeolites, Naples" (L. V. C. Rees, Ed.), p. 607. Heyden, London, 1980.
- Guisnet, M., Alvarez, F., Gianetto, G., and Perot, G., *Catal. Today* **1**, 433 (1987).
- Kim, J.-Ho, Tanabe, M., and Niwa, M., *Micro. Mater.* **10**, 85 (1997).
- Stull, D. R., Westrum, E. F., Jr., and Sinke, G. C., in "The Chemical Thermodynamics of Organic Compounds." Wiley & Sons, New York, 1969.
- Germain, J. E., in "Catalytic Conversion of Hydrocarbons." Academic Press, London, 1969.
- Miale, J. N., Chen, N. Y., and Weisz, P. B., *J. Catal.* **6**, 278 (1966).